

Classification of A Terrestrial Laser Scanner Point Cloud of A Conifer Forest Using Object-based Image Analysis

Maeta N.¹ and Matsuoka M.^{1*}

¹Graduate School of Engineering, Mie University, 1577, Kurima-machiya, Tsu, Mie 514-8597, Japan

*matsuoka@info.mie-u.ac.jp

Abstract A Terrestrial Laser Scanner (TLS) is an efficient tool for measuring the size, number and distribution of trees in artificial forests. The Forestry Agency of Japan has promoted the use of remote sensing technology to solve forestry-related problems such as the aging of the workforce. Classification of the TLS point cloud into trees parts (trunks, branches, and leaves) plays an important role in estimating the volume of forest resources, measuring the timber growth, and the three-dimensional (3D) modeling of tree shapes. However, the accurate classification of the 3D point clouds of conifer forests is still challenging issue. One difficulty is to represent the relationships between points in 3D space. Therefore, we propose a novel approach of classification. It is based on object-based image classification to images generated by projecting point clouds onto a plane. The purpose of this study is to investigate the feasibility of this approach. The point cloud data was obtained in a conifer forest in the Experiment Forest of the Graduate School of Bioresources, Mie University in Mie Prefecture, Japan. The point cloud was projected onto a cylindrical plane centered on the TLS based on elevation and azimuth angles. This resulted in panoramic image-like data. Each pixel has 12 features related to the points, including reflected intensity and distance from the TLS and maximum difference from neighboring points. The Orfeo Toolbox was used to manipulate the image objects, i.e. the groups of connected pixels. Object-based image classification was applied to the segmented images to classify them into trees parts and ground. As a result, some branch objects were correctly classified, but others were incorrectly classified as leaves. This approach can be applied as a new classification method. We expect this approach to be most appropriate for the original TLS data, which has a radial point cloud coordinate centered on the instrument. We plan to compare this method with other classification methods to confirm its effectiveness.

Keywords: conifer forest, machine learning, Object-based Image Analysis, point cloud, Terrestrial Laser Scanner

Introduction/ Background

The Japanese forestry industry is facing some of challenges related to the workforce, including a decline in the number of workers. The number of forestry workers has declined over the past 40 years. The Forestry Agency of Japan (2020) reported that the workforce has

decreased by approximately one-third over the course of this period. Under these circumstances, the Forestry Agency of Japan has been encouraging the use of remote sensing technologies with the aim of reducing operational costs. These technologies include the Light Detection and Ranging (LiDAR) as a Terrestrial Laser Scanner (TLS), satellite data from Landsat and Sentinel, and aerial imagery captured by an Unmanned Aerial Vehicle (UAV). These remote sensing data could be analyzed to extract various forest attributes such as tree height, diameter, and number of trees. These measurements are of great importance during both harvesting and shipping operations as timber product. Furthermore, most of the artificial forests in Japan are conifers (mainly cedar and cypress), making them worthy of study. Considering these aspects, remote sensing technologies would be very useful for accurately assessing the shape and condition of coniferous trees. The TLS is particularly suitable for more detailed measurements of conifer structure. It allows measurements from the side with less interference from the canopy. The TLS has been widely studied in other tree-related fields, such as classifying tree parts using deep learning (Yang et al. 2024) and researching combined with the satellite data (Matsuoka et al. 2020). The TLS is very useful for research because of its flexibility with an increasing demand for its application. In recent years, TLS has become a very important tool in the pursuit of work efficiency in forestry operations.

Problem Statement

To evaluate the shape and condition of conifers, it is necessary to classify trees into parts (trunks, branches, leaves). Because the size, usage, and other characteristics vary greatly depending on the parts of the tree. Therefore, classification of the TLS point cloud into trees parts plays an important role in forestry industry. For example, the volume of forest resources can be estimated from branches and trunks size. We can also measure wood growth by acquiring and comparing the data continuously. Moreover, three-dimensional (3D) modeling of tree shapes can be applied to various simulations. However, the accurate classification of the 3D point clouds of a conifer forest is still challenging issue. One difficulty is to represent the relationships between points in 3D space. This problem could be solved by determining the interconnection of neighboring points with respect to the parts of the tree. However, the definition of “neighboring point” is also ambiguous in 3D.

Objective

We propose a new classification approach to address above mentioned problem about the relation of points. This approach treats point cloud data as a two-dimensional (2D) image projected onto a plane, and performs object-based classification based on the image. Each image pixel is individually classified based on the object it belongs to, then the pixel is transformed back into a point cloud in the original 3D space to reconstruct the 3D data. This process has the advantage of efficiently using spatial relationships with neighboring points that are difficult to obtain directly in 3D space. It is therefore expected to contribute to improved classification accuracy and reduced processing time. In addition, there is a greater degree of freedom for 3D viewing and analysis. The objective of this study is to evaluate the feasibility and validity of this approach and to investigate further improvements and potential applications.

Literature Review

Fol et al. (2023) evaluated the performance of TLS compared to four different 3D data acquisition methods - close-range photogrammetry, fish-eye photogrammetry, mobile laser scanning, and mixed reality depth camera. This was driven by the fact that TLS had been the primary method for producing highly accurate 3D models of forests for many years, leading to the exploration of alternative acquisition methods. The TLS remained effective for obtaining 3D point cloud data of forests.

Eto et al. (2020) investigated methods for classifying trees parts with high accuracy based on features such as the significant difference in reflected intensity between leaves and branches. In order to acquire tree features, it is necessary to properly separate the trunks, leaves, and branches from the point cloud. Therefore, they applied the machine learning methods, Random Forest (RF) and k-means clustering, to classify the point cloud. The trunks were determined by whether the shapes were in circular or oval when the point cloud was sliced in parallel to the ground. Leaves and branches were classified by RF using labels and abstracted features. The result was high accuracy RF classification of branches and leaves. They found that the trunks had the characteristic of being cylindrical shape perpendicular to the ground. The trunks were detected by this characteristic. They also found that leaves and branches can be classified with high accuracy using trained machine learning. In their study, the classification was performed in the state of a 3D point cloud.

Liu et al. (2021) evaluated an approach to reconstruct tree geometry using a neural network called the Tree Part Net. The method was applied to the point cloud of hardwood trees. This method takes advantage of the assumption that trees are composed of local cylindrical shapes,

applied primarily to branches. They showed the effectiveness of the method in reconstructing the full 3D tree model geometry. An approach based on the characteristics of trees parts, such as the cylindrical shape of branches, is considered to be effective for trees parts classification. Xu et al. (2023) studied the geometric registration of the TLS point cloud, specifically TLS to TLS registration and TLS and the Airborne Laser Scanner registration. TLS can obtain more information if it can be registered with other observations using remote sensing technologies. For other studies, Saito et al. (2017) created a 2D image with a point cloud, and Onodera & Masuda (2015) matched the laser reflected intensity to the camera image.

Methodology

a. Analysis Flow:

Figure 1 shows the workflow in this study. In TLS data acquisition, we describe TLS data acquisition. It mainly contains information about the location where the acquisition was performed and the status of the acquisition. In image generation, we describe the process of generating the 2D image and information about the generated 2D image. In this study, 12 features have been assigned and an additional process was applied to our data to reduce the pixel gap in the generated image. In Object-based Image Analysis (OBIA) segmentation, we describe object-based segmentation. Labeling was also performed during this process. In SVM classification, we describe the classification using SVM. In the results and discussion, we evaluate the classification result mainly by the visual interpretation.

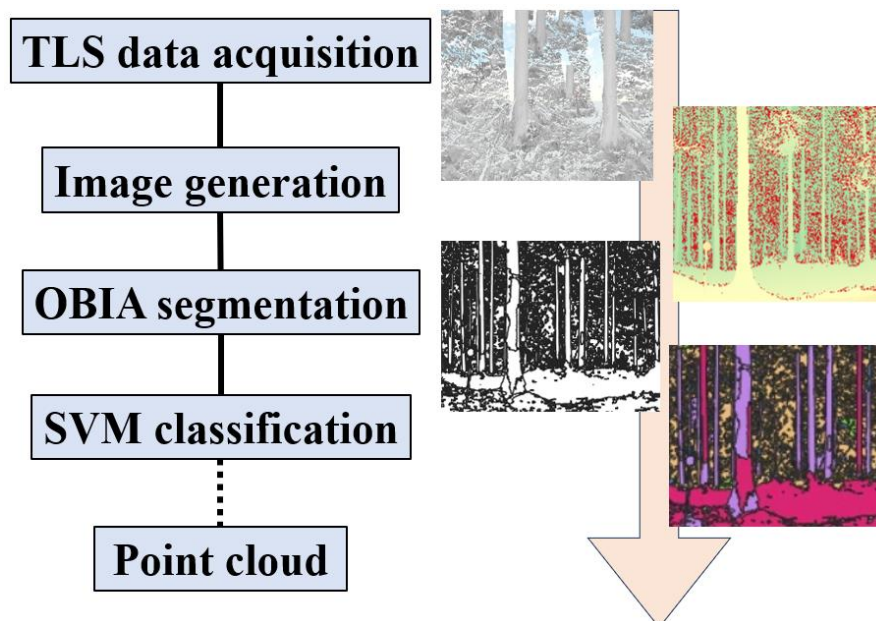


Figure 1: Data Analysis Flow

b. TLS Data Acquisition:

The point cloud was acquired in a conifer forest in the Hirakura Experimental Forest of the Graduate School of Bioresources, Mie University. Figure 2 shows the location of the Hirakura Experimental Forest. It is located at Misugi Town, Tsu City, Mie Prefecture, Japan (N34°27' E136°14'). Figure 3 shows a photograph of the measurement. The target trees were conifers (cedar and cypress) and about 30 meters tall. We were able to measure almost the entire part of the tree except for the top of the tree behind the canopy. Measurements were made on October 11 from 10:00 to 17:00 and on October 12 from 10:00 to 14:00. The weather was clear on both days. The TLS acquires a point cloud by emitting a laser beam and detecting the reflected beam as it rotates 360 degrees around the instrument. We usually operate the TLS to scan the target from several surrounding positions to reduce the shadow of the beam and capture more detail. The data acquired from multiple scan positions is registered using reference spheres distributed around the target area. The approach in this study should be applied to the point cloud of a single scan because the point cloud will be reprojected onto the cylindrical plane centered on the instrument. Table 1 is the summary of the measurement settings, and Figure 4 shows a picture of the TLS. We used FARO Focus3D X330 (FARO 2024). The acquisition was conducted at three sites in the Experimental Forest, five scans at each location. At the time of measurement, eight reference spheres were placed at each location. For accurate registration, the TLS was placed in a position where at least 5 spheres could be scanned. With a resolution of 1/2 and a quality of 4x, approximately 173 million points were acquired in approximately 30 minutes.

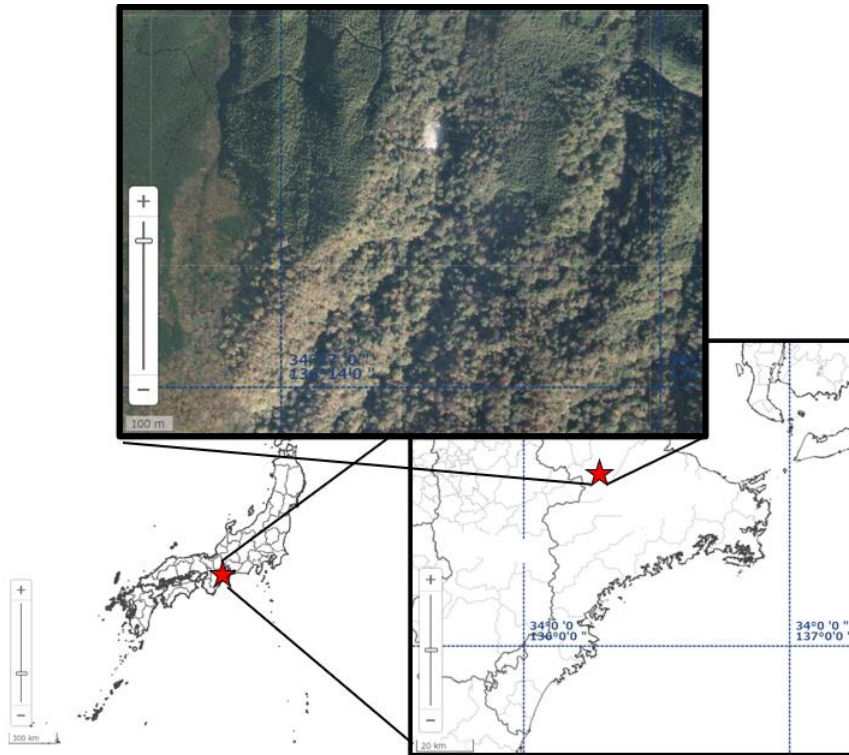


Figure 2: Location of the Data Acquisition Site, Hirakura Experimental Forest



Figure 3: Measurement Picture



Figure 4: TLS Picture (FARO Focus3D X330)

Table 1: Acquisition Details

Product Name	FARO Focus3D X330		
Resolution	1/2	Quality	4x
Observe Point	Num. of site 5	Reference Sphere	Num. of sphere 8

c. Generation of 2D image:

The acquired point cloud data were converted into files that could be processed by programming languages using FARO SCENE software. In our data, every point has (x, y, z) coordinates and two types of reflected intensity. In the conversion to a 2D image, all points were projected onto a cylindrical plane centered on the TLS based on elevation and azimuth angles. The elevation and azimuth angles were calculated by transforming the 3D Cartesian coordinates into the 3D polar coordinates, as shown in the following equation:

$$r = \sqrt{x^2 + y^2 + z^2}$$

$$\theta = \cos^{-1} \frac{z}{r}$$

$$\varphi = \text{sgn}(y) \cos^{-1} \frac{x}{\sqrt{x^2 + y^2}}$$

where r is the distance from TLS ($r > 0$), θ is the azimuth angle of TLS ($-180 < \theta \leq 180$), φ is the elevation angle ($-90 < \varphi \leq 90$), (x, y, z) are the Cartesian coordinates, and $\text{sgn}()$ is the signum function, respectively.

The variables of azimuth and elevation angle were transformed into a 2D image by arranging them in sequence on a plane centered at zero. The result was saved as image file

in TIF format. The image looks similar to the panoramic image shown in Figure 5. Each pixel in this image represents individual TLS points.





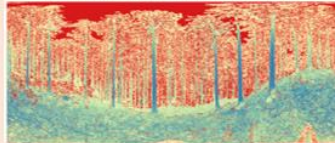
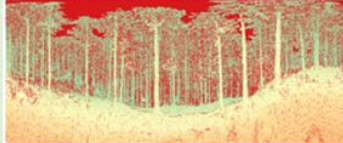








Figure 5: Generated 2D Image (Distance)

Twelve features were assigned to each pixel. These features and pictures are shown in Table 2. Five variables x , y , z , reflection intensity 1, and reflection intensity 2 are the features acquired during the TLS measurement and represent the Cartesian coordinates and reflected intensity. The variable “distance from TLS” was the same as r in above equation calculated during the polar coordinate transformation. Another five features were generated from above distance image. The variables “pixel variance (3×3)” and “pixel variance (5×5)” indicate the variance of distance calculated using 3×3 and 5×5 pixels around the center pixel, respectively. The variable “maxi. difference in distance from neighboring points” was the largest absolute distance between the center and the surrounding four pixels in the top, bottom, left, and right directions. This was used to more clearly represent 3D boundaries that are difficult to represent on a 2D plane. The variable “maxi. difference in distance from horizontal neighboring points” was largest absolute difference between the center and the surrounding two pixels in the left and right direction. This was used to clearly represent cylindrical features with different directions, such as trunks and branches. The variable “maxi. difference in distance from vertical neighboring points” was the largest absolute difference between the center and the surrounding two pixels in the top and bottom. This was used to clearly express the characteristics of the state of something associated with a horizontal cylindrical shape, such as a branch and leaves. “Data availability” was the index whether the pixel has valid (1) data or not (0). Sky does not have point cloud information, for example.

Finally, all features were multiplied by “data availability” as a mask image. These processes were performed in Python using the rasterio module (Mapbox 2024). The rasterio module is a library for reading, manipulating, and exporting raster data. This is because the rasterio module is based on the Geospatial Data Abstraction Library (GDAL, <https://gdal.org/>), which is characterized by its ability to perform coordinate transformations and projective system operations.

Table 2: Assigned 12 Features

x-coordinate 	y-coordinate 	z-coordinate 
reflectance intensity 1 	reflectance intensity 2 	distance from observation 
pixel variance (3x3) 	pixel variance (5x5) 	data availability 
Maxi. difference distance from neighboring points 	Maxi. difference distance from horizontal neighboring points 	Maxi. difference distance from vertical neighboring points 

d. OBIA Segmentation:

The Orfeo Toolbox (OTB) (2024), the plugin tool of QGIS (2024), was used to manipulate the image objects i.e. the groups of connected pixels. The segmentation function of OTB was used to divide all pixels into the number of segments. The segmentation was conducted using the Mean Shift Algorithm. This is an algorithm that moves data points along a gradient of density and aggregates them at the location (mode) with the highest density. Each data point converges to the same mode through a process of repeated motion and clustering. It is suitable when the number of objects is large because the number of clusters does not need to be determined in advance. Furthermore, this algorithm is suitable when clusters of different shapes can be created. The algorithm was selected because we wanted to treat objects with similar characteristics as the same object, and because the image size is very large.

Figure 6 shows an example of segmentation results. Each area bounded by a black line is an

object. Objects vary in size, even in the same tree part. Each parameter was determined manually by running the function several times and checking the segmentation results. The resulting parameters used are shown in Table 3. The other parameters are set by default. The "Spatial Radius" specifies the spatial search area. The "Range Radius" specifies the range within which the similarity of the features should be considered. The "Minimum Object Size" is a parameter to specify the minimum cluster size. The "Tile Size" is a parameter that specifies the size of the image when it is divided into small tiles for processing. Finally, image was segmented into approximately 60,000 objects, and it was saved in SHP format.



Figure 6: Generated by the Segmentation

Table 3: Segmentation Parameter

Spatial Radius	Range Radius	Minimum Object Size	Tile Size
10 pixels	30 pixels	10 pixels	512 pixels

e. SVM Classification:

First, we labeled the trees parts to the segments using QGIS to be used for the training and evaluation of the classification. Five labels were given: "trunks, branches, leaves, soil, and no-data". Figure 7 shows the results of labeling. Labeled files are overlaid on segmented files. In total, approximately 400 objects were labeled. Table 4 shows the number of each label. The number of labels for soil and no data is small because they are supplemental object classes. Branches and leaves were labeled especially more than the other categories because their boundaries are ambiguous. The understory vegetations were also labeled as soil. Although we still have a subjective aspect, the labeling was done as objectively as possible. This labeled SHP file is used as training data.

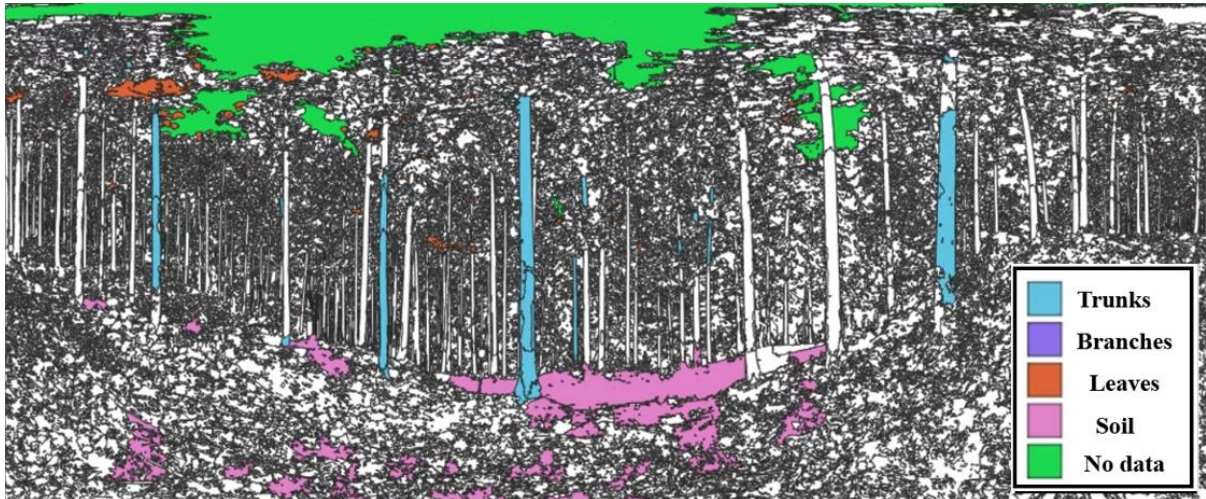



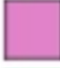



Figure 7: Labeled Objects for Training

Table 4: Number of Labels

Label	No.
 Trunks	59
 Branches	86
 Leaves	215
 Soil	29
 No data	15

Subsequently, each object was assigned features using OTB's Zonal Statistics. Table 5 shows the new features assigned to the object were the mean, the standard deviation, the maximum, the minimum, and the sum calculated from the above 12 features using the pixels belonging to the object. In total, 60 features (12×5) are assigned to the image object. Classification is performed based on these features.

Table 5: Assigned 5 Features

sum	maximum	minimum
mean	standard deviation	

Training was performed using OTB's Train Vector Classifier. The classification model was used a Support Vector Machine (SVM). Because SVM was the most accurate, when we performed pixel-based classification in preliminary experiment. Training used the default SVM parameters.

Finally, the learned classification model was applied to the entire segment using OTB's Vector Classifier. We conducted in a different field than the one we had already labeled. We applied it to all the objects.

f. Supplementary Processing in 2D Image Generation:

In this study, additional corrections were made to simplify the main line. It was the reduction of image resolution by half to fill the gap of 2D image. Processing was as follows. If there is a data in the top left pixel, replace that pixel as the output pixel. If there is a data in any of the four pixels other than the top left pixel, replace that pixel as the output pixel. If all four pixels are no data, replace that pixel as no data. This process has been performed for all pixels. According to the original specifications, this process is not necessary. This is because of the entire image is composed of filled pixels. However, we wanted to remove the noise to eliminate its effect on the features. In addition, the excessive processing time was also an issue in this study. Consequently, we were able to remove a lot of noise and compress the size down to 1/4 of its original size.

Results and Discussion

Figure 8 shows the SVM classification results in different colors. Although this is a qualitative assessment, approximately half of the objects were successfully classified. Branches and leaves appear to be relatively correct compared to the others. The large number of these labels may also have had an effect. The classification results differed from the labeled results in some labeled areas. This was because the training had not been done well. On the other hand, objects classified as branches were often correct as branches. However, some areas that should have been classified as branches were also misclassified as leaves. In addition, some trunks objects were misclassified as soil. Furthermore, several areas of no data were also misclassified as soil. These are because the boundaries of the objects were not completely separated during the segmentation stage. It could be improved by examining the segmentation parameters again and changing to an object with clearer boundaries. There were also a few objects that had anomalous straight line segmentation. We believe this is due to the tile size of the segmentation parameter. Therefore, increase the tile size value. When labeling, there should also be approximately 400 labels for correct answers as well as labels for training. This is intended to provide a quantitative evaluation of the classification results instead of a qualitative one.

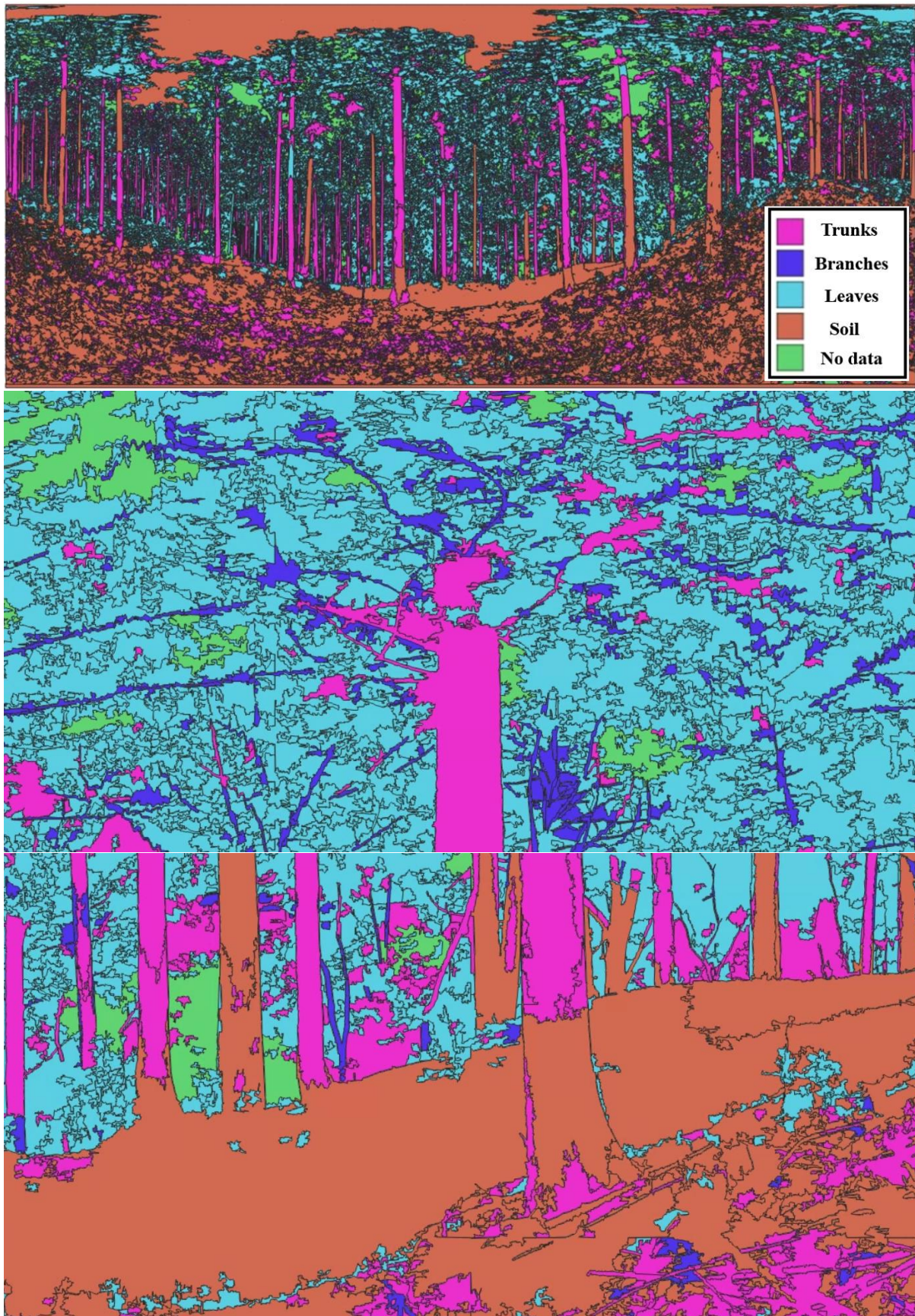


Figure 8: Classification Result. Top: entire image, middle: enlarged view of canopy, and bottom: enlarged view of floor.

Conclusion and Recommendation

We have investigated an approach that takes several novel perspectives on 3D point cloud classification and confirmed that classification can be performed. The first perspective is a method that projects a point cloud into 2D and performs classification by considering the feature values of neighboring points. The second perspective is to perform 2D object-based image classification on point clouds. These approaches have shown the potential to become a valuable classifier, even given the current results. The effectiveness of this method is expected. This is because many 3D point cloud classifications have not been performed on data that is not aligned. The effectiveness of this method is expected, because many 3D point cloud classifications are not performed on data that has not been registered. In the future, we are planning a phase to further validate the effectiveness of this method. First, we will confirm this using a confusion matrix to quantitatively evaluate. Second, permutation feature importances are performed to evaluate which features have a significant impact on classification. Based on the object labels, pixels are then labeled and returned to the 3D point cloud. We also plan to compare this method with other classification methods to confirm its effectiveness. This research has the potential to improve the effectiveness of forestry operations. However, this approach can be extended to areas other than forestry, and further development is expected. Furthermore, integrating the sequence of operations into point cloud processing software could yield significant commercial benefits.

Acknowledgement

This research has been conducted in collaboration with the Hirakura Experimental Forest, Faculty of Bioresources, Mie University.

References

- Dimitrios, P., Azadeh, A., & Martin, S. (2022). 3D point cloud fusion from UAV and TLS to assess temperate managed forest structures. *International Journal of Applied Earth Observation and Geoinformation*. Vol. 112, No. 7. <https://doi.org/10.1016/j.jag.2022.102917>
- Eto, S., & Masuda, H. (2020). Extraction and Evaluation of Tree Traits Using TLS Point Clouds. *The 2020 Spring Conference of the Japan Society for Precision Engineering*, pp. 228-229, 17-19 March 2020, Tokyo, Japan. https://doi.org/10.11522/pscjspe.2020S.0_228
- FARO. (n.d.). FARO industries. Accessed on September 13, 2024, to

<https://www.faro.com/>

Fol, C. R., Kükenbrink, D., Rehus, N., Murtiyoso, A., & Griess, V. C. (2023). Evaluating State-of-the-art 3D Scanning Methods for Stem-level Biodiversity Inventories in Forests. *International Journal of Applied Earth Observation and Geoinformation*, Vol. 122, No. 1. <https://doi.org/10.1016/j.jag.2023.103396>

Forestry Agency of Japan. (2020). Report on the demonstration of harvest survey using a ground-based 3D laser scanner (in Japanese). Retrieved June 18, 2024, from https://www.rinya.maff.go.jp/j/gyoumu/gijutu/attach/pdf/syuukaku_kourituka-58.pdf

Liu, Y., Guo, J., Benes, B., Deussen, O., Zhang, X., & Huang, H. (2021). TreePartNet: Neural Decomposition of Point Clouds for 3D Tree Reconstruction. *ACM Transactions on Graphics*. Vol. 40, No. 6, pp1-16. <https://dl.acm.org/doi/abs/10.1145/3478513.3480486>

Mapbox. rasterio. Retrieved May, 22, 2024, from <https://rasterio.readthedocs.io/en/stable/>

Matsuoka, M., Moriya, H., & Yoshioka, H. (2020). Correction of Canopy Shadow Effects on Reflectance in an Evergreen Conifer Forest using a 3D Point Cloud. *Remote Sensing*, Vol. 12, No. 14, pp. 2178. <https://doi.org/10.3390/rs12142178>

Onodera, R., & Masuda, H. (2015). Correction Method for Colored Point Clouds Using Laser Reflectance Intensity. *The 2015 Spring Conference of the Japan Society for Precision Engineering*, pp. 503-504, 27-29 March 2015, Tokyo, Japan. https://doi.org/10.11522/pscjspe.2015S.0_503

Orfeo Toolbox. (n.d.). Retrieved July, 26, 2024, from <https://www.orfeo-toolbox.org/>

QGIS. QGIS. Retrieved April, 26, 2023, from <https://www.qgis.org/>

Saito, K., Hiraoka, Y., Masuda, H., Matsushita, M., & Takahashi, M. (2017). Tree Shape Generation Method for Forests Using Large-scale Point Cloud Data. *The 128th Annual Meeting of the Japanese Forest Society*, pp. 26-29, 27-29 March 2017, Kagoshima, Japan. https://doi.org/10.11519/jfsc.128.0_47

Xu, N., Qin, R., & Song, S. (2023). Point Cloud Registration for LiDAR and Photogrammetric Data: A Critical Synthesis and Performance Analysis on Classic and Deep Learning Algorithms. *ISPRS Open Journal of Photogrammetry and Remote Sensing*, vol. 8, No. 1, pp. 28-43. <https://doi.org/10.1016/j.ophoto.2023.100032>

Yang, X., Miao, T., Tian, X., Wang, D., Zhao, J., Lin, L., Zhu, C., Yang, T., & Xu, T. (2024). Maize stem-leaf segmentation framework based on deformable point clouds. *ISPRS Journal of Photogrammetry and Remote Sensing*, Vol. 211, No. 1, pp. 49-66. <https://doi.org/10.1016/j.isprsjprs.2024.03.025>